

## Displaying Digital Deep Sky Images

Emmanuel Bertin<sup>1</sup>

<sup>1</sup>*Institut d'Astrophysique de Paris, UMR 7095 CNRS, Université Pierre et Marie Curie, 98<sup>bis</sup> Boulevard Arago, F-75014 Paris, France*

**Abstract.** In Astronomy, many activities such as survey data quality visual control, crowd-sourced projects, atlas publishing and outreach initiatives require digital images of the deep sky to be displayed in a legible and consistent way for both professional and more general audiences. Important technical facts about display devices and standards are unfortunately unknown to most professional astronomers and the appearance of published images is often unsatisfactory as a result of a questionable trial-and-error approach. In this short paper I discuss the main technical issues one faces when displaying astronomical images in various contexts. I propose some guidelines as well as a software implementation, the STIFF package, to automate the process of providing consistent, ready-for-use pictures directly from science image data.

### 1. Introduction

Preparing astronomical pictures of the deep sky for display has long been considered something of a black art. Chemical photography probably earned this reputation out of the difficulties to deal with characteristic curves and to master photo-chemical processes. But some twenty years plus into the era of digital cameras, we must recognise the fact that most of us still follow a trial-and-error approach while preparing astronomical pictures for publications or web galleries. Although powerful interactive tools such as ds9<sup>1</sup> (Joye & Mandel 2003) or the FITS LIBERATOR<sup>2</sup> (Nielsen et al. 2008) makes this tuning process an enjoyable and creative experience, they can hardly be used for creating thousands or millions of thumbnails of galaxies, e.g., for an on-line image database (e.g., Baillard et al. 2011). In this short article we propose some ingredients of a recipe for preparing astronomical pictures of the deep sky in an automated way, that combines both fidelity to the original signal and legibility of the image content, leaving aside aesthetic considerations. More details can be found in the documentation that accompanies the STIFF software package, available from the ASTROMATIC website<sup>3</sup>, and which implements most of the ideas presented here.

---

<sup>1</sup><http://hea-www.harvard.edu/RD/ds9>

<sup>2</sup>[http://www.spacetelescope.org/projects/fits\\_liberator](http://www.spacetelescope.org/projects/fits_liberator)

<sup>3</sup><http://astromatic.net/software/stiff>

## 2. Intensity mapping

The main issue one faces when displaying a astronomical image is how to translate pixel values from the science data files into grey levels. There is a widespread misconception that the 8-bit representation used in video buffers and in file formats such as JPEG, PNG or TIFF (“display formats”), follows the same rule as in scientific formats like FITS, namely that raw pixel values are linearly related to surface brightness. Most image display/preparation applications get round this by providing “stretch functions” that compress the dynamic range in luma (e.g., Lupton et al. 2004). But in reality, display formats are “gamma-compressed”. Gamma compression was originally a direct consequence of the non-linear relation existing between light intensity and voltage in Cathode Ray Tubes (CRTs). CRT screens have a natural response function  $I' \propto p^\gamma$ , with  $\gamma \approx 2.2$  and where  $p$  is the input pixel value and  $I'$  the displayed intensity. Although display technology has evolved, all modern display devices still perform (or at least emulate) gamma expansion, which has therefore to be compensated for before data being stored in a display format. In practice, several constraints with the display of real images (perceptual contrast matching, presence of ambient light, signal-to-noise ratio limitations, and colour-space conversion issues) have led engineers to alter the simple reverse law  $p = I^{1/\gamma}$ , where  $0 \leq I < 1$  is the normalised recorded intensity, and define instead

$$p = \begin{cases} a.I & \text{if } 0 \leq I < I_t \\ (1+b).I^{1/\gamma} - b & \text{if } I_t \leq I \leq 1 \end{cases}, \quad (1)$$

where the  $\gamma$ ,  $a$ ,  $b$  and  $I_t$  parameters can take different values depending on the encoding standard (Fig 1); for example in the sRGB standard  $\gamma = 2.4$ ,  $a = 12.92$ ,  $b = 0.055$  and  $I_t = 0.00304$ .

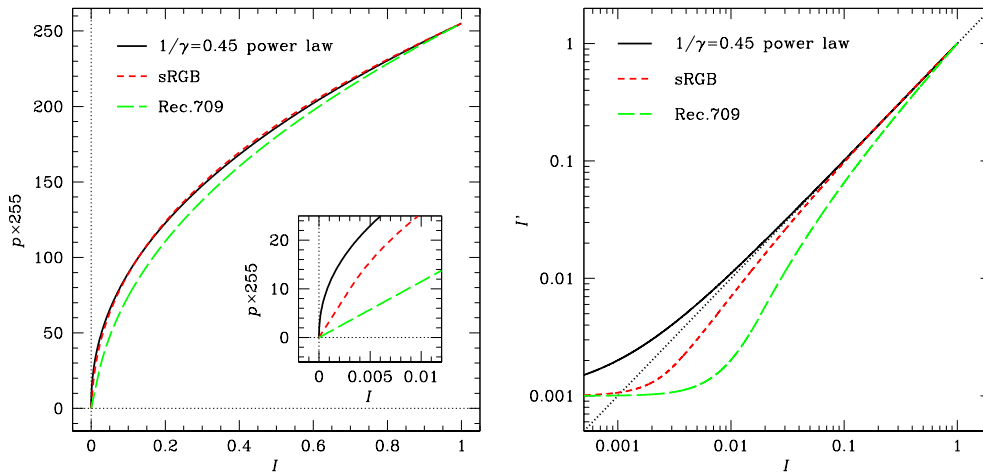


Figure 1. Three types of gamma compression. *Left*: encoded pixel values (for an 8-bit image) vs relative original image intensity; *black curve (continuous)*: pure power law, *red (short dashes)*: sRGB, *green (long dashes)*: ITU-R Rec. BT.709. Note the important difference at low intensities (*insert*). *Right*: Comparison between the end-to-end transfer curves, assuming a 2.2 display gamma and a minimum black level at 0.1% of full white.

Thanks to the gamma compression/expansion mechanism, a fair fraction of the dynamic range of modern imaging instruments ( $\approx 90$  dB) can be fit over 256 levels of grey (8 bits) without the need of an external stretch function (Fig. 2).

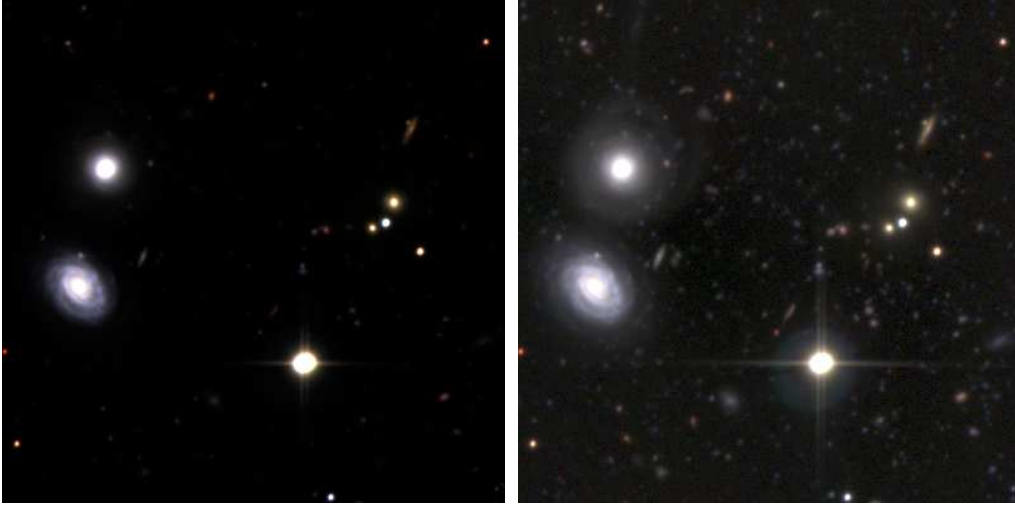


Figure 2. The same deep-sky image processed with (right) and without (left) gamma compression, using the same surface brightness cuts.

### 3. Surface brightness cuts

Surface brightness cuts  $f_{\min}$  and  $f_{\max}$  are used to normalise the recorded intensity  $I$  before it is gamma-compressed in (1):  $I = (f - f_{\min}) / (f_{\max} - f_{\min})$ , where  $f$  is the surface brightness from the pixel values stored in the science image file. Deep exposures taken at high galactic latitude are generally dominated by a flat, noisy sky background with variable amplitude  $f_{\text{sky}}$ . To provide a consistent rendering of images, we force the sky background to be displayed as a fixed dark grey  $I' = \rho_{\text{grey}}$ , and choose a surface brightness upper limit  $f_{\max}$  which will be displayed as full white ( $I' = 1$ ). We get

$$f_{\min} = \frac{f_{\text{sky}} - \rho_{\text{grey}} f_{\max}}{1 - \rho_{\text{grey}}}, \quad (2)$$

where  $f_{\text{sky}}$  is the sky background level measured in the science images. A  $\rho_{\text{grey}}$  of about 0.1 % is appropriate for pictures intended to be displayed on computer monitors in controlled light environments. In low density regions of the sky, reasonable values for  $f_{\text{sky}}$  and  $f_{\max}$  can be obtained simply from quantiles of the surface brightness distribution (the 50th and 99th percentiles for instance).

### 4. Colour mapping

Mixing astronomical images taken through two or more filters to create colour pictures brings precious visual clues about the spectral content of sources. But without

further processing, colours of stars and galaxies observed through contiguous broadband optical filters look deceptively dull. To increase the colour saturation of images while maintaining the luma and global white balance, we can replace — before gamma-compression — the  $(R, G, B)$  triplet of normalised red, green, blue primary colour components with  $(R_\alpha, G_\alpha, B_\alpha)$  such that

$$\begin{aligned} R_\alpha &= Y + \alpha \frac{2R - G - B}{3}, \\ G_\alpha &= Y + \alpha \frac{2G - R - B}{3}, \end{aligned} \quad (3)$$

$$B_\alpha = Y + \alpha \frac{2B - R - G}{3}, \quad (4)$$

where  $Y = (R + G + B)/3$  is the luma of the normalised image.  $\alpha$  acts exactly like the saturation knob of a colour TV: for  $\alpha = 0$ , the three channels are combined to form a black-and-white (greyscale) image;  $\alpha = 1$  lets the input colour saturation unchanged, while  $\alpha > 1$  exaggerates the colours. Fig. 3 shows the effect of changing  $\alpha$  on a deep-sky colour image. For images taken in contiguous channels,  $\alpha = 2.0$  generally gives best results.

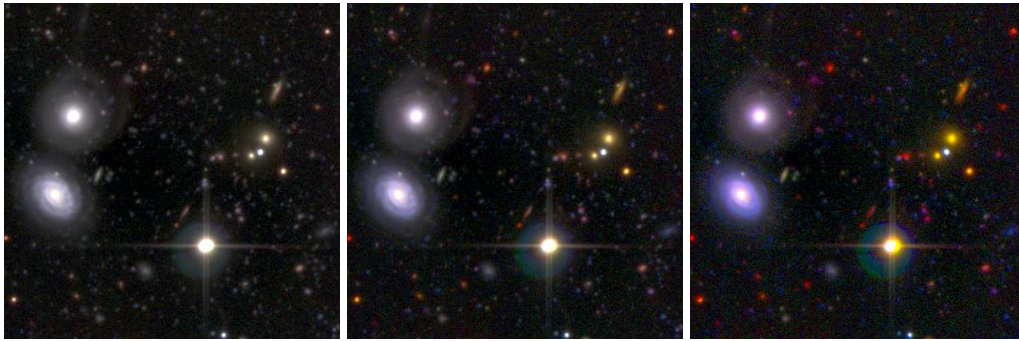


Figure 3. A three-channel deep-sky image processed with three different values of the colour saturation parameter  $\alpha$ . From *left to right*: 1.0, 2.0 and 4.0.

## References

- Baillard, A., Bertin, E., de Lapparent, V., Fouqué, P., Arnouts, S., Mellier, Y., Pelló, R., Leborgne, J.-F., Prugniel, P., Makarov, D., Makarova, L., McCracken, H. J., Bijaoui, A., & Tasca, L. 2011, *A&A*, 532, A74. 1103.5734
- Joye, W. A., & Mandel, E. 2003, in *Astronomical Data Analysis Software and Systems XII*, edited by H. E. Payne, R. I. Jedrzejewski, & R. N. Hook, vol. 295 of *Astronomical Society of the Pacific Conference Series*, 489
- Lupton, R., Blanton, M. R., Fekete, G., Hogg, D. W., O’Mullane, W., Szalay, A., & Wherry, N. 2004, *PASP*, 116, 133. [arXiv:astro-ph/0312483](https://arxiv.org/abs/astro-ph/0312483)
- Nielsen, L. H., Christensen, L. L., Hurt, R. L., Nielsen, K., & Johansen, T. 2008, in *Communicating Astronomy with the Public*, edited by L. L. Christensen, M. Zoulias, & I. Robson, 486